Human Reproduction, Vol.38, No.3, pp. 387–399, 2023
Advance Access Publication on January 16, 2023 https://doi.org/10.1093/humrep/dead001

human reproduction

ORIGINAL ARTICLE *Embryology*

Maternal age affects pronuclear and chromatin dynamics, morula compaction and cell polarity, and blastulation of human embryos

Kenji Ezoe [1], Tetsuya Miki [1], Hikari Akaike [1], Kiyoe Shimazaki [1], Tsubasa Takahashi [1], Yuko Tanimura [1], Ayumi Amagai [1], Ayano Sawado [1], Mai Mogi [1], Shigeru Kaneko [1], Satoshi Ueno [1], Giovanni Coticchio [2], Danilo Cimadomo [3], Andrea Borini [2], Laura Rienzi [3,4], and Keiichi Kato [1,*]

[1]Kato Ladies Clinic, Tokyo, Japan [2]9.baby, GeneraLife IVF, Bologna, Italy [3]Clinica Valle Giulia, GeneraLife IVF, Rome, Italy [4]Department of Biomolecular Sciences, University of Urbino "Carlo Bo", Urbino, Italy

*Correspondence address. Kato Ladies Clinic, 7-20-3 Nishishinjuku, Shinjuku-ku, Tokyo 160-0023, Japan. Tel: +81-3-3366-3777; Fax: +81-3-3366-3908; E-mail: k-kato@towako.net https://orcid.org/0000-0002-1394-4532

Submitted on October 20, 2022; resubmitted on December 7, 2022; editorial decision on January 3, 2023

STUDY QUESTION: Does maternal ageing impact early and late morphokinetic and cellular processes of human blastocyst formation?

SUMMARY ANSWER: Maternal ageing significantly affects pronuclear size and intra- and extra-nuclear dynamics during fertilization, dysregulates cell polarity during compaction, and reduces blastocoel expansion.

WHAT IS KNOWN ALREADY: In ART, advanced maternal age (AMA) affects oocyte yield, fertilization, and overall developmental competence. However, with the exception of chromosome segregation errors occurring during oocyte meiosis, the molecular and biochemical mechanisms responsible for AMA-related subfertility and reduced embryo developmental competence remain unclear. In particular, studies reporting morphokinetics and cellular alterations during the fertilization and pre-implantation period in women of AMA remain limited.

STUDY DESIGN, SIZE, DURATION: A total of 2058 fertilized oocytes were stratified by maternal age according to the Society for Assisted Reproductive Technology classification (<35, 35–37, 38–40, 41–42, and >42 years) and retrospectively analysed. AMA effects were assessed in relation to: embryo morphokinetics and morphological alterations; and the presence and distribution of cell polarity markers—Yes-associated protein (YAP) and protein kinase C-ζ (PKC-ζ)—involved in blastocyst morphogenesis.

PARTICIPANTS/MATERIALS, SETTING, METHODS: A total of 1050 cycles from 1050 patients met the inclusion criteria and were analysed. Microinjected oocytes were assessed using a time-lapse culture system. Immature oocytes at oocyte retrieval and mature oocytes not suitable for time-lapse monitoring, owing to an excess of residual corona cells or inadequate orientation for correct observation, were not analysed. Phenomena relevant to meiotic resumption, pronuclear dynamics, cytoplasmic/cortical modifications, cleavage patterns and embryo quality were annotated and compared among groups. Furthermore, 20 human embryos donated for research by consenting couples were used for immunofluorescence.

MAIN RESULTS AND THE ROLE OF CHANCE: Static microscopic observation revealed that blastocyst formation and expansion were impaired in the 41–42 and >42-year groups ($P < 0.0001$). The morphological grades of the inner cell mass and trophectoderm were poorer in the >42-year group than those in the <35-year group ($P = 0.0022$ and $P < 0.0001$, respectively). Time-lapse microscopic observation revealed a reduction in nucleolus precursor body alignment in female pronuclei in the 41–42 and >42-year groups ($P = 0.0010$). Female pronuclear area decreased and asynchronous pronuclear breakdown increased in the >42-year group ($P = 0.0027$ and $P < 0.0122$, respectively). Developmental speed at cleavage stage, incidence of irregularity of first cleavage, type and duration of blastomere movement, and number of multinucleated cells were comparable among age groups. Delayed embryonic compaction and an increased number of extruded blastomeres were observed in the >42-year group ($P = 0.0002$ and $P = 0.0047$, respectively). Blastulation and blastocyst expansion

were also delayed in the 41–42 and >42-year groups ($P < 0.0001$ for both). YAP positivity rate in the outer cells of morulae and embryo PKC-ζ immunoflourescence decreased in the >42-year group ($P < 0.0001$ for both).

LIMITATIONS, REASONS FOR CAUTION: At the cellular level, the investigation was limited to cell polarity markers. Cell components of other developmental pathways should be studied in relation to AMA.

WIDER IMPLICATIONS OF THE FINDINGS: The study indicates that maternal ageing affects the key functions of embryo morphogenesis, irrespective of the well-established influence on the fidelity of oocyte meiosis.

STUDY FUNDING/COMPETING INTEREST(S): This study was supported by the participating institutions. The authors have no conflicts of interest to declare.

TRIAL REGISTRATION NUMBER: N/A.

Key words: blastocyst / cell polarity / compaction / fertilization / maternal age / morphokinetics / nucleolus precursor body / pronuclear / protein kinase C-ζ / Yes-associated protein

Introduction

Human reproductive success is highly dependent on parental age, especially maternal, when attempting to conceive (Mills *et al.*, 2011; Schmidt *et al.*, 2012). As women age, the probability of pregnancy and live birth substantially decreases owing to a reduction in both the quantity and quality of oocytes, leading to increased risks of infertility, miscarriages, and birth defects (Mosher and Pratt, 1991; Heffner, 2004; ESHRE Capri Workshop Group, 2008; Duncan *et al.*, 2017). In ART, maternal age is the strongest predictor of pregnancy and obstetric outcomes (Nelson and Lawlor, 2011). Advanced maternal age (AMA) has deleterious effects on oocyte retrieval, fertilization, and above all embryonic ploidy (Franasiak *et al.*, 2014; Capalbo *et al.*, 2017; Abe *et al.*, 2020; Bebbere *et al.*, 2022). Furthermore, developmental competence at pre-implantation stages is reduced with AMA (Mazzilli *et al.*, 2017; Ubaldi *et al.*, 2017). However, with the exclusion of chromosome segregation errors affecting oocyte meiosis (Gruhn *et al.*, 2019), the molecular and biochemical mechanisms involved in AMA-related infertility and their impact on developmental competence remain unclear (Cimadomo *et al.*, 2018; Bebbere *et al.*, 2022).

Mitochondrial dysfunction also contributes to the AMA effect (Diez-Juan *et al.*, 2015). In fact, mitochondrial activity, which is physiologically activated only at the blastocyst stage (Van Blerkom, 2011), declines with advancing age in oocytes (Keefe *et al.*, 1995; Ramalho-Santos *et al.*, 2009) and embryos at the morula stage (Morimoto *et al.*, 2020). Previous studies have also reported that the blastocyst formation rate declined owing to an increase in embryo arrest at the morula stage in women of AMA (Janny and Menezo, 1996; Pantos *et al.*, 1999). Although these deleterious effects of AMA are possibly reflected in developmental events during fertilization, cleavage, compaction, and blastulation, studies reporting embryo morphokinetics and morphological alterations in women of AMA are limited. Several authors reported increased abnormal cleavage and delayed blastulation and expansion of embryos from women of AMA (Kirkegaard *et al.*, 2016; Barrie *et al.*, 2021; Lebovitz *et al.*, 2021). However, the evidence on the impact of AMA on embryo development remains controversial (Faramarzi *et al.*, 2019; Warshaviak *et al.*, 2019; Barrie *et al.*, 2021; Lebovitz *et al.*, 2021). Furthermore, the correlation between AMA and morphokinetics during fertilization and compaction was not assessed in previous studies, despite these stages significantly reflecting developmental competence and pregnancy outcomes (Lagalla *et al.*, 2017; Coticchio *et al.*, 2018; Ezoe *et al.*, 2020; Lagalla *et al.*, 2020; Coticchio *et al.*, 2021b; Ezoe *et al.*, 2022a). Therefore, this study aimed at revealing the impact of maternal ageing on cellular events, as revealed by morphokinetic analysis, during human fertilization and embryonic development, especially during compaction. We also assessed the possible influence of AMA on the expression of cell polarity markers, Yes-associated protein (YAP) and protein kinase C-ζ (PKCζ) (Coticchio *et al.*, 2019; Gerri *et al.*, 2020), during blastomere compaction. We specifically focused on this developmental interval because it represents a crucial transition, when developmental errors—potentially relevant to maternal age—and associated attempts of correction may emerge.

Materials and methods

Ethical approval

This study was approved by the Institutional Review Board of Kato Ladies Clinic on 30 March 2021 (approval number: 21-21). Written informed consent for the analysis was obtained from all patients.

Patients

The treatment records of women undergoing oocyte retrieval after clomiphene citrate (CC)-based minimal stimulation cycles at the Kato Ladies Clinic between October 2019 and December 2020 were reviewed. Patients requiring surgical sperm retrieval and/or those with recurrent implantation failure, i.e. experiencing four or more unsuccessful embryo transfers (ETs), were excluded (Coughlan *et al.*, 2014) (Supplementary Fig. S1). Only the first oocyte retrieval of each eligible patient treated during the study period was included in the analysis to avoid possible bias from patient background. Patients were categorized by maternal age according to the classification of the Society for Assisted Reproductive Technology (<35, 35–37, 38–40, 41–42 and >42 years), (Toner *et al.*, 2016). The immature oocytes at the oocyte retrieval and seven mature oocytes not suitable for time-lapse monitoring, owing to an excess of residual corona cells (n = 1) or inadequate orientation for correct observation (n = 6), were not analysed.

CC-based minimal ovarian-stimulation cycle IVF

A detailed protocol for minimal stimulation with CC has been previously reported (Kato *et al.*, 2018; Karakida *et al.*, 2020). Briefly, CC

(50–100 mg/day; Fuji Pharma Co., Ltd., Tokyo, Japan) was administered according to an extended regimen from Day 3 of the cycle until the induction of the final oocyte maturation. Ultrasound and hormonal monitoring were initiated on Day 8 and performed daily until ovulation was triggered. When the size of the dominant follicle developed to larger than 18 mm, ovulation was triggered by the GnRH agonist buserelin via the nasal route (Suprecur; Mochida Pharmaceutical Co., Ltd., Tokyo, Japan or Buserecur; Fuji Pharma Co., Ltd.).

Oocyte retrieval was performed between 34 and 36 h after the trigger using a 21 G needle (Kitazato Corporation, Shizuoka, Japan). Cumulus–oocyte complexes were collected, washed and cultured in human tubal fluid (HTF) medium (Kitazato Corporation) with paraffin oil at 37°C (gas phase: 5% O_2, 5% CO_2 and 90% N_2) until denudation before ICSI (Ezoe *et al.*, 2020).

Semen was collected by self-stimulated ejaculation as sperm samples, and washed by centrifugation (600 × *g*, 15 min) with 70% and 90% density gradients (Isolate; Irvine Scientific, Santa Ana, CA, USA). The prepared sperm samples were cultured in HTF medium at 37°C (gas phase: 5% O_2, 5% CO_2 and 90% N_2) until use.

ICSI and embryo culture

Oocytes were inseminated by ICSI in HEPES-buffered HTF medium (Ohata *et al.*, 2019). The injected oocytes were immediately placed in EmbryoSlides (Vitrolife, Inc., Göteborg, Sweden) and cultured individually in 180 µl medium (SAGE 1-Step; CooperSurgical, Inc., Måløv, Denmark) overlaid with paraffin oil. Embryos were cultured at 37°C (gas phase: 5% O_2, 5% CO_2 and 90% N_2) in an Embryoscope + time-lapse incubator (Vitrolife) for 5–7 days. Fertilization was observed using the EmbryoViewer software (Vitrolife).

Annotation and assessment of embryo development

Images were captured after every 10 min at 11 focal planes over 5–7 days of culture. The time points for the onset of the following events were recorded and analysed: second polar body extrusion, cytoplasmic wave (tCW), appearance of female and male pronuclei (PNs), PN juxtaposition, breakdown of PNs, nucleolus precursor body (NPB) alignment in the PNs, start of the 2-cell (t2), 3-cell (t3), 4-cell (t4), 5-cell (t5), 6-cell (t6), 7-cell (t7) and 8-cell (t8) stages, initiation of compaction (tSC), completion of compaction process (tM), initiation of blastulation (tSB), and formation of full (tB) and expanded (tEB) blastocysts (Coticchio *et al.*, 2018; ESHRE Working group on Time-lapse technology, 2020). Female and male PN were discriminated based on: mutual positions and relative to the second polar body; and positional association with the CW (Coticchio *et al.*, 2018; Ezoe *et al.*, 2022d). The presence and timing of the cytoplasmic halo during fertilization was also annotated, as reported previously (Ezoe *et al.*, 2020, 2021b). Briefly, the time of halo initiation (tHa) was first identified by cytoplasmic granule movement towards the centre of ooplasm. The time of the end of this centripetal movement (tHc) was recorded. After central repositioning, granules began to move back to the cortex. The tHr as the time when the granules started to redistribute, and tHd as the time when the halo phenomenon disappeared were recorded. PN juxtaposition and PN breakdown synchrony were annotated as previously reported (Ezoe *et al.*, 2022a). When trichotomous mitosis was observed, embryos exhibited direct cleavage (Kola *et al.*, 1987). When the time interval (TI) between t2 and t3 was <5 h, embryos exhibited rapid cleavage (Rubio *et al.*, 2012; Ciray *et al.*, 2014). Asymmetrical divisions during the first cell division and reverse cleavage were recorded. The type (bouncing, wobbling and twist-and-crumble) and duration of blastomere movement at the first cleavage were annotated as previously reported (Ezoe *et al.*, 2019; Ohata *et al.*, 2019). The duration of blastomere movement at the two-cell stage was annotated, and the ratio of blastomere movement duration to two-cell stage duration was calculated. The number of multinucleated cells and amount of fragmentation in the cleavage stage were annotated (Ezoe *et al.*, 2022c). During the embryo peri-compaction period, excluded/extruded cells were identified only when they clearly displayed the presence of nuclei, as previously described (Coticchio *et al.*, 2021b). Morula and blastocyst qualities were evaluated according to Ebner's criteria (Ebner *et al.*, 2009) and Gardner's criteria (Gardner and Schoolcraft, 1999), respectively. All annotations in the Embryo Viewer software and conventional morphological grading of embryos were performed by nine operators, each with >5 years of experience in embryology, who were blinded to the patient characteristics and clinical outcomes. In preparation for the present study, operators observed 30 fertilized oocytes and developed the criteria for annotation. The inter- and intra-operator variation in times of second polar body extrusion, the appearance of female and male PNs and initiation of compaction, which have been reported to be difficult to annotate consistently (Sundvall *et al.*, 2013; Martinez *et al.*, 2018), were assessed using 10 additional fertilized oocytes. The intraclass correlation coefficient can be interpreted as follows: 0–0.20, poor agreement; 0.21–0.40, fair agreement; 0.41–0.60, moderate agreement; 0.61–0.80, strong agreement; and >0.81, almost perfect agreement.

Blastocyst warming and transfer

Blastocyst warming was performed using Cryotop (Kitazato Corporation), as described previously (Mori *et al.*, 2015; Ohata *et al.*, 2021). Briefly, the Cryotop was placed into a warming solution of 1.0 M sucrose at 37°C for 1 min. Subsequently, the blastocysts were removed from the warming solution and transferred to a diluent solution of 0.5 M sucrose at room temperature. After 3 min, they were transferred to the washing solution without sucrose. For final dilution, blastocysts were transferred to the washing solution for 1 min.

Monitoring included transvaginal ultrasonography and blood hormone testing. Ovulation was triggered using buserelin (Suprecur; Mochida Pharmaceutical Co., Ltd., Tokyo, Japan or Buserecur; Fuji Pharma Co., Ltd.) after confirming initiation of the LH surge. Blastocysts were selected according to their developmental speed and morphological grade (Kato *et al.*, 2014), and single vitrified-warmed blastocyst transfers (SVBTs) were performed (Kato *et al.*, 2018). Dydrogesterone (30 mg/day) was administered orally during the early luteal phase after SVBT. In addition, in cases with insufficient luteal function (progesterone level on the day of SVBT <11 ng/ml), progesterone was administered intravaginally (Lutinus, Ferring Pharmaceuticals, Saint Prex, Switzerland) until the ninth week of pregnancy. Implantation was defined by serum hCG level (>20 IU/ml), in accordance with a previous study (Ueno *et al.*, 2014). The clinical and

ongoing pregnancy rates were defined according to the ultrasonographic observation of a gestational sac 3 weeks after SVBTs and the observation of a foetal heartbeat 5 weeks after SVBTs, respectively. Live birth was defined as delivery at ≥22 weeks of pregnancy. Early pregnancy loss and miscarriage were defined according to the absence of a gestational sac after implantation as well as the absence of live birth after the confirmation of a gestational sac (Ezoe *et al.*, 2022b).

Immunofluorescence for Yap and PKCζ

In total, 20 discarded, vitrified human embryos donated for research by consenting couples who conceived babies and completed the fertility treatment were examined for YAP and PKCζ protein [young group (<35 years), n = 10; AMA group (>42 years), n = 10] (Supplementary Table SI). These embryos were vitrified on Day 2 for the vitrified-warmed cleavage stage ETs. The donated embryos were warmed using the Cryotop method mentioned above and cultured at 37°C (gas phase: 5% O_2, 5% CO_2 and 90% N_2) in an Embryoscope + time-lapse incubator (Vitrolife) for 48 h. Analysis by immunofluorescence was performed as previously described (Ezoe *et al.*, 2021a). Embryos were fixed in 4% neutral-buffered formalin (Sigma Aldrich, St Louis, MO, USA) for 60 min, washed three times in wash buffer [0.1% Triton X-100 (Sigma Aldrich) in PBS (Sigma Aldrich)], blocked [3% bovine serum albumin (Sigma Aldrich) in PBS], incubated for 16 h with primary antibodies in blocking buffer, washed and stained with labelled secondary antibodies (Supplementary Table SII) and Hoechst 33342 (Sigma Aldrich). As a negative control, embryos were incubated with isotype-specific immunoglobulin and stained with labelled secondary antibodies and Hoechst 33342 (Supplementary Table SII). Embryos were imaged using a BZ-X800 fluorescence microscope (Keyence, Osaka, Japan). The fluorescence intensity was measured using the BZ-X800 Analyzer software (Keyence). Briefly, the fields were selected for observation, and the average intensity of the fields was automatically calculated. The experiments were repeated at least 10 times.

Statistical analyses

Statistical analyses were performed using the JMP software (SAS, Cary, NC, USA). Proportions of the data were analysed using the chi-squared test and Fisher's exact test. Continuous parameters were compared using Student's *t*-test or one-way ANOVA, and significance was determined using Tukey's test for *post hoc* analysis when normality could be accepted; otherwise, Mann–Whitney *U* test was used. The Spearman rank correlation test was used to measure the degree of association between two continuous variables. Univariate logistic regression analysis was performed to identify confounders that were potentially associated with the outcomes. Furthermore, the association of the covariates with the groups was analysed. Multivariate logistic regression analysis and multivariate linear regression analysis were performed to adjust for bias (using the confounders and covariates) and verify the statistical significance (Supplementary Table SIII). Adjusted odds ratios are reported with 95% CIs for each group. $P < 0.05$ was considered statistically significant.

Results

Patient characteristics and embryonic outcomes assessed by static microscopic observation

A total of 1050 cycles from 1050 patients met the inclusion criteria and were analysed. Patient characteristics are shown in Table I. Male age and female BMI significantly increased with female age ($P < 0.0001$ and $P < 0.0001$, respectively). The concentration of motile sperm was different among age groups ($P = 0.0002$). Embryo developmental rates were comparable among all age groups during the cleavage and compaction stages (Table I). However, the blastocyst formation rate was significantly decreased in the 41–42 and >42-year groups ($P < 0.0001$); their developmental rate to the expanded blastocyst stage was further decreased in the >42-year group as compared to that in the 41–42-year group. The multivariate logistic regression analysis demonstrated an AMA-related decrease in blastocyst expansion (Supplementary Table SIV).

Morphokinetics

Inter- and intra-observer agreements for the investigated parameters are shown in Supplementary Table SV, with almost perfect agreement obtained for all parameters.

Fertilization

The correlation between female age and fertilization events was extensively analysed (Table II). The timing of both female and male PN appearance was comparable among the age groups. The presence and timing of the CW and halo were comparable among the groups. The incidence and timing of PN juxtaposition were comparable among the groups. The area of female PN was significantly decreased in the >42-year group ($P = 0.0122$), and the incidence of NPB alignment in the female PN was also decreased in the 41–42 and >42-year groups ($P = 0.0010$). However, the area of male PN and its incidence of NPB alignment were comparable among groups. Although the timing of female and male PN breakdown was comparable among groups, the incidence of asynchronous breakdown increased in the >42-year group ($P = 0.0027$); the female PN disappeared earlier in most cases in all groups (60–100%). These correlations were also confirmed by the multivariate regression analysis (Supplementary Tables SIV and SVI).

Early cleavage stages

The developmental speed, incidence of irregularity of first cleavage, type and duration of blastomere movement, and number of multinucleated cells were comparable among the age groups (Supplementary Table SVII). Furthermore, the morphological grades on Days 2 and 3 were comparable among the groups.

Table I Patient characteristics and embryo outcomes.

Age group	<35 years	35–37 years	38–40 years	41–42 years	>42 years	*P* value
No. of patients	158	193	294	198	207	
Maternal age (years)	32.4 ± 0.1[a]	36.1 ± 0.0[b]	39.1 ± 0.0[c]	41.5 ± 0.0[d]	43.9 ± 0.0[e]	<0.0001*
Paternal age (years)	35.1 ± 0.2[a]	38.5 ± 0.2[b]	41.5 ± 0.2[c]	43.5 ± 0.2[d]	45.7 ± 0.2[e]	<0.0001*
No. of previous oocyte retrieval cycles	1.9 ± 0.1	1.8 ± 0.1	1.8 ± 0.0	1.9 ± 0.1	2.0 ± 0.1	0.1860*
No. of previous embryo transfer cycles	1.3 ± 0.1	1.5 ± 0.1	1.4 ± 0.1	1.3 ± 0.1	1.3 ± 0.1	0.2558*
BMI (kg/m^2)	20.7 ± 0.2[a]	21.0 ± 0.2[a,b]	21.5 ± 0.2[a,b]	21.7 ± 0.2[b,c]	22.4 ± 0.2[c]	<0.0001*
Infertility cause						0.2576**
Ovulation, n (%)	2 (1.3)	9 (4.7)	4 (1.4)	5 (2.5)	3 (1.5)	
Tubal factor, n (%)	3 (1.9)	7 (3.6)	15 (5.1)	9 (4.6)	2 (1.0)	
Endometriosis, n (%)	3 (5.7)	6 (3.1)	8 (2.7)	4 (2.0)	7 (3.4)	
Endometrial factor, n (%)	10 (6.3)	11 (5.7)	12 (4.1)	8 (4.0)	8 (3.9)	
Male factor, n (%)	59 (37.3)	63 (32.6)	89 (30.3)	69 (34.9)	81 (39.1)	
Combined, n (%)	20 (12.7)	33 (17.1)	49 (16.7)	30 (15.2)	33 (15.9)	
Unexplained, n (%)	55 (34.8)	64 (33.2)	117 (39.8)	73 (36.9)	73 (35.3)	
Sperm concentration (M/ml)	45.3 ± 3.4	51.4 ± 2.9	56.8 ± 2.7	55.5 ± 3.3	50.8 ± 2.9	0.0742*
Motile sperm (M/ml)	20.8 ± 1.9[a,b]	25.4 ± 1.8[c]	25.7 ± 1.4[c]	24.3 ± 2.1[a,c]	19.3 ± 1.7[b]	0.0002*
Abnormal sperm (M/ml)	44.4 ± 3.3	50.3 ± 2.8	54.2 ± 2.6	53.0 ± 3.2	49.2 ± 2.7	0.1621*
No. of zygotes, n	309	386	572	372	419	
No. of 2-cell stage embryos, n (%)	308 (99.7)	380 (98.5)	566 (99.0)	370 (99.5)	412 (98.3)	0.2964**
No. of 3-cell stage embryos, n (%)	306 (99.0)	377 (97.7)	564 (98.6)	368 (98.9)	410 (97.9)	0.4513**
No. of 4-cell stage embryos, n (%)	306 (99.0)	373 (96.6)	558 (97.6)	365 (98.1)	409 (97.6)	0.3109**
No. of 5-cell stage embryos, n (%)	302 (97.7)	370 (95.9)	548 (95.8)	363 (97.6)	407 (97.1)	0.3441**
No. of 6-cell stage embryos, n (%)	300 (97.1)	367 (95.1)	546 (95.5)	362 (97.3)	405 (96.7)	0.3577**
No. of 7-cell stage embryos, n (%)	294 (95.2)	363 (94.0)	539 (94.2)	353 (94.9)	403 (96.2)	0.6371**
No. of 8-cell stage embryos, n (%)	290 (93.9)	358 (92.8)	530 (92.7)	346 (93.0)	400 (95.5)	0.4204**
No. of morulae, n (%)	255 (82.5)	329 (85.2)	484 (84.6)	311 (83.6)	346 (82.6)	0.7893**
No. of blastocysts, n (%)	233 (75.4)[a]	289 (74.9)[a]	415 (72.6)[a]	246 (66.1)[b]	252 (60.1)[b]	<0.0001**
No. of expanded blastocysts, n (%)	221 (71.5)[a]	274 (71.0)[a]	376 (65.7)[a]	211 (56.7)[b]	206 (49.2)[c]	<0.0001**

Values are presented as mean ± SEM or n (%).
[a–e]Different superscript letters indicate a significant difference at $P < 0.05$.
*Mann–Whitney *U* test.
**Chi-squared test.

Morula and blastocyst stages

Delayed embryonic compaction was observed in the >42-year group ($P = 0.0002$, Table III). Blastulation and blastocyst expansion were also delayed in the 41–42 and >42-year groups ($P < 0.0001$ for both). The TIs from t8 to tSC and from tB to tEB were prolonged with increasing female age ($P = 0.0140$ and $P = 0.0006$, respectively). These correlations were confirmed using the multivariate regression analysis (Supplementary Table SVI).

The TI from t8 to tSC was divided in quartiles; the proportion of embryos in the upper quartile was significantly higher in the >42-year group than in the other groups ($P < 0.0001$, Supplementary Table SVIII). Furthermore, TI from t8 to tSC was significantly associated with subsequent development; both early (<11.5) and delayed (≥25.9) compaction adversely affected blastocyst formation and expansion ($P < 0.0001$, Supplementary Table SIX). Both shortening and prolongation of TI from t8 to tSC were also associated with impaired morphology of the inner cell mass (ICM) and trophectoderm (TE).

The morphological grade at 92 h post-insemination was significantly impaired in the 41–42 and >42-year groups (Table III). Although the number of excluded blastomeres was not altered by female ageing, the number of extruded blastomeres after compaction significantly increased in the >42-year group. The proportion of partially compacted morula with extruded blastomeres increased as female age increased. The morphological grades of ICM and TE were significantly poorer in the >42-year group. These correlations were confirmed using the multivariate regression analysis (Supplementary Table SIV).

Pregnancy outcomes after SVBTs

The rates of implantation, clinical pregnancy, ongoing pregnancy, and live birth were significantly decreased as the maternal age increased

Table II Morphokinetics during fertilization.

Age group	<35 years	35–37 years	38–40 years	41–42 years	>42 years	*P* value
No. of zygotes, n	309	386	572	372	419	
Time of second polar body extrusion	3.0 ± 0.0	3.1 ± 0.0	3.0 ± 0.0	3.1 ± 0.0	3.1 ± 0.0	0.5040*
Time of CW	4.5 ± 0.1	4.6 ± 0.1	4.5 ± 0.0	4.6 ± 0.1	4.6 ± 0.1	0.2031*
Zygotes with CW, n (%)	309 (100)	383 (99.2)	572 (100)	372 (100)	419 (100)	0.1522**
Time of appearance of male PN (h)	4.7 ± 0.1	4.9 ± 0.1	4.8 ± 0.0	5.0 ± 0.1	4.9 ± 0.1	0.0716*
Time of appearance of female PN (h)	5.0 ± 0.1	5.2 ± 0.1	5.1 ± 0.1	5.2 ± 0.1	5.2 ± 0.1	0.1944*
Time of halo appearance (h)	7.9 ± 0.1	7.9 ± 0.1	8.0 ± 0.1	8.1 ± 0.1	8.2 ± 0.1	0.2008*
Zygotes with cytoplasmic halo, n (%)	303 (98.1)	374 (96.9)	565 (98.8)	366 (98.4)	410 (97.9)	0.3297**
Time of PN juxtaposition (h)	9.0 ± 0.2	9.1 ± 0.2	9.0 ± 0.1	8.8 ± 0.1	9.2 ± 0.2	0.5426*
Time of halo centring (h)	12.4 ± 0.2	12.5 ± 0.1	12.6 ± 0.1	13.0 ± 0.1	13.0 ± 0.1	0.0579*
Time of NPB alignment in female PN (h)	12.6 ± 0.3	12.8 ± 0.3	12.3 ± 0.2	12.9 ± 0.3	12.4 ± 0.3	0.5171*
Zygotes with NPB alignment in female PN, n (%)	236 (76.4)[a]	269 (69.7)[a]	409 (71.5)[a,b]	250 (67.2)[b,c]	268 (64.0)[c]	0.0010**
Time of NPB alignment in male PN (h)	16.4 ± 0.4	17.0 ± 0.4	16.6 ± 0.3	16.5 ± 0.4	16.1 ± 0.3	0.4421*
Zygotes with NPB alignment in male PN, n (%)	150 (48.5)	160 (41.5)	237 (41.4)	145 (39.0)	181 (43.2)	0.1344**
Time of halo redistribution (h)	20.5 ± 0.2	20.5 ± 0.2	20.4 ± 0.1	20.9 ± 0.2	20.4 ± 0.2	0.2247*
Time of halo disappearance (h)	23.1 ± 0.2	23.1 ± 0.2	23.1 ± 0.1	23.5 ± 0.2	23.1 ± 0.2	0.3109*
Area of female PN (μm^2)	543.6 ± 4.7[a]	538.0 ± 4.3[a,b]	534.2 ± 3.6[a,b]	531.6 ± 4.1[a,b]	522.4 ± 4.4[b]	0.0122*
Area of male PN (μm^2)	613.5 ± 5.7	609.2 ± 5.7	607.7 ± 4.3	607.7 ± 4.8	605.8 ± 5.1	0.7061*
Zygotes with PN juxtaposition immediately before breakdown, n (%)	296 (95.8)	366 (94.8)	545 (95.3)	349 (93.8)	393 (93.8)	0.6440**
Time of female PN breakdown (h)	23.1 ± 0.2	23.3 ± 0.2	23.2 ± 0.2	23.5 ± 0.2	23.2 ± 0.3	0.7063*
Time of male PN breakdown (h)	23.1 ± 0.2	23.2 ± 0.2	23.2 ± 0.2	23.7 ± 0.2	23.3 ± 0.3	0.4430*
Zygotes with asynchronous PN breakdown (TI between PN breakdowns < 1 h), n (%)	1 (0.3)[a]	3 (0.8)[a]	7 (1.2)[a]	6 (1.6)[a,b]	15 (3.6)[b]	0.0027**
PN disappeared earlier						
Female PN, n (%)	1 (100)	2 (66.7)	6 (85.7)	5 (83.3)	9 (60.0)	0.6391**
Male PN, n (%)	0 (0)	1 (33.3)	1 (14.3)	1 (16.7)	6 (40.0)	

Values are presented as mean ± SEM or n (%).
CW: cytoplasmic wave; PN: pronuclear; NPB: nucleolus precursor body.
[a–c]Different superscript letters indicate a significant difference at $P < 0.05$.
*Mann–Whitney *U* test.
**Chi-squared test.

($P < 0.0001$ for all, Supplementary Table SX). The multivariate logistic regression analysis also demonstrated the AMA-related decrease in live birth probability (Supplementary Table SXI). Furthermore, the positive correlation was observed between the miscarriage rate and maternal age ($P < 0.0001$) although the rate of early pregnancy loss was comparable among the groups ($I = 0.7461$, Supplementary Table SX).

Yap and PKCζ in human morula stage embryos

All embryos survived after warming and no degenerated blastomeres were observed in both the young age group (<35 years) and AMA group (>42 years, Supplementary Table SI). Although the developmental rate to the morula stage was comparable between the groups, a delay in cell proliferation and embryonic compaction was observed in the AMA group ($P = 0.0003$ and $P = 0.0085$, respectively; Supplementary Table SI). The presence of YAP and PKCζ was examined by immunofluorescence (Fig. 1). The number of YAP-positive cells in the outer cells of the morulae was significantly higher in the young age group than in the AMA group ($P < 0.0001$, Fig. 1a and b). A similar distribution of PKCζ protein was observed in both age groups (Fig. 1a). PKCζ fluorescence intensity was higher in the cortical region of the outer cells than in the central region or inner cells (Fig. 1a and c). However, PKCζ fluorescence intensity in the cortical region of morulae was significantly lower in the AMA group than in the young age group (Fig. 1d). The total cell number was not correlated with YAP-positive rate (Spearman's rank correlation coefficient, 0.3511; $P = 0.1118$) and PKCζ fluorescence intensity (Spearman's rank correlation coefficient, 0.3727; $P = 0.1056$).

Discussion

We demonstrated that AMA significantly affected the rates of blastocyst formation and expansion. However, the developmental rates during cleavage and compaction were comparable among all age groups.

Table III Morphokinetics at morula and blastocyst stage of human embryos.

Age group	<35 years	35–37 years	38–40 years	41–42 years	>42 years	*P* value
No. of morulae, n	255	329	484	311	346	
Timing of embryo development to each stage						
tSC (h)	76.1 ± 0.5[a]	76.4 ± 0.5[a]	77.7 ± 0.5[a,b]	78.4 ± 0.6[a,b]	79.2 ± 0.6[b]	0.0002*
tM (h)	85.4 ± 0.6[a]	85.9 ± 0.6[a]	86.7 ± 0.5[a,b]	88.3 ± 0.6[b,c]	88.8 ± 0.6[c]	<0.0001*
tSB (h)	95.7 ± 0.5[a]	96.8 ± 0.5[a]	97.3 ± 0.5[a,b]	99.2 ± 0.6[b,c]	99.7 ± 0.6[c]	<0.0001*
tB (h)	106.9 ± 0.7[a]	109.6 ± 0.7[a,b]	108.9 ± 0.6[a,b,c]	111.4 ± 0.9[b,c]	112.0 ± 0.8[c]	<0.0001*
tEB (h)	116.5 ± 0.8[c]	118.7 ± 0.8[a,b]	118.8 ± 0.7[a,b]	120.8 ± 0.9[b,c]	124.2 ± 1.1[c]	<0.0001*
Time intervals between each stage						
From t8 to tSC (h)	18.6 ± 0.6[a]	18.7 ± 0.5[a]	18.8 ± 0.5[a]	19.4 ± 0.6[a,b]	20.9 ± 0.5[b]	0.0140*
From tSC to tM (h)	9.7 ± 0.4	9.7 ± 0.3	9.8 ± 0.3	10.3 ± 0.3	10.5 ± 0.3	0.2812*
From tM to tSB (h)	10.5 ± 0.5	11.2 ± 0.4	11.3 ± 0.4	11.4 ± 0.4	12.3 ± 0.5	0.1042*
From tSB to tB (h)	11.6 ± 0.4	13.3 ± 0.4	12.4 ± 0.4	13.4 ± 0.6	13.3 ± 0.5	0.0574*
From tB to tEB (h)	10.5 ± 0.4[a]	10.4 ± 0.4[a]	11.5 ± 0.3[a,b]	12.0 ± 0.5[b]	12.7 ± 0.6[b]	0.0006*
Developmental stage at 92 h post-insemination						
Before compaction, n (%)	6 (2.4)	16 (4.9)	21 (4.3)	22 (7.1)	21 (6.1)	0.0957**
After compaction, n (%)	200 (78.4)	250 (76.0)	388 (70.2)	250 (80.4)	289 (83.5)	0.1742**
After blastulation, n (%)	3 (19.2)[a]	63 (19.2)[a]	75 (15.5)[a,b]	39 (12.5)[b,c]	36 (10.4)[c]	0.0045**
Morphological grade at 92 h post-insemination						
C1, n (%)	74 (37.0)	97 (38.8)	145 (37.4)	96 (38.4)	105 (36.3)	0.9775**
C2, n (%)	29 (14.5)	41 (16.4)	64 (16.5)	40 (16.0)	38 (13.2)	0.7602**
C3, n (%)	73 (36.5)[a]	78 (31.2)[a,b]	132 (34.0)[a]	60 (24.0)[b]	84 (29.1)[a,b]	0.0299**
C4, n (%)	24 (12.0)[a]	34 (13.6)[a]	47 (12.1)[a]	54 (21.6)[b]	62 (21.5)[b]	0.0005**
Exclusion of blastomeres before compaction						0.7213**
No blastomere, n (%)	154 (60.4)	215 (65.4)	310 (64.1)	197 (63.4)	223 (64.5)	
1 blastomere, n (%)	28 (11.0)	34 (10.3)	53 (11.0)	37 (11.9)	49 (14.2)	
2 blastomeres, n (%)	26 (10.2)	30 (9.1)	42 (8.7)	20 (6.4)	26 (7.5)	
3 blastomeres, n (%)	20 (7.8)	14 (4.3)	24 (5.0)	20 (6.4)	17 (4.9)	
≥4 blastomeres, n (%)	27 (10.6)	36 (10.9)	55 (11.4)	37 (11.9)	31 (9.0)	
Extrusion of blastomeres after compaction						
No blastomere, n (%)	199 (78.0)[a]	235 (71.4)[a,b,c]	358 (74.0)[a,b]	217 (69.8)[b,c]	224 (64.7)[c]	0.0047**
1 blastomere, n (%)	27 (10.6)	39 (11.9)	61 (12.6)	35 (11.3)	49 (14.2)	0.6944**
2 blastomeres, n (%)	6 (2.4)	21 (6.4)	25 (5.2)	21 (6.8)	18 (5.2)	0.1623**
≥3 blastomeres, n (%)	23 (9.0)[a]	34 (10.3)[a]	40 (8.3)[a]	38 (12.2)[a,b]	55 (15.9)[b]	0.0080**
Pattern of compaction						
FCM, n (%)	129 (50.6)	159 (48.3)	251 (51.9)	145 (46.6)	157 (45.4)	0.3569**
Exc-PCM, n (%)	70 (27.5)	76 (23.1)	107 (22.1)	72 (23.2)	67 (19.4)	0.2283**
Ext-PCM, n (%)	25 (9.8)[a]	56 (17.0)[b,c]	59 (12.2)[a,b]	52 (16.7)[b,c]	66 (19.1)[b,c]	0.0053**
Exc/Ext-PCM, n (%)	31 (12.2)	38 (11.6)	67 (13.8)	42 (13.5)	56 (16.2)	0.4586**
Morphological grade of inner cell mass						
Grade A, n (%)	116 (54.2)	131 (49.3)	163 (45.2)	92 (46.9)	73 (39.7)	0.0593**
Grade B, n (%)	61 (28.5)	67 (25.2)	122 (34.4)	54 (27.6)	54 (29.4)	0.1420**
Grade C, n (%)	37 (17.3)[a]	68 (25.6)[b,c]	70 (19.7)[a,b]	50 (25.5)[b,c]	57 (31.0)[c]	0.0065**
Morphological grade of trophectoderm						
Grade A, n (%)	108 (50.5)[a]	110 (41.4)[b]	143 (40.3)[b]	79 (40.3)[b]	52 (28.3)[c]	0.0004**
Grade B, n (%)	44 (20.6)	59 (22.2)	92 (25.9)	45 (23.0)	43 (23.4)	0.6522**
Grade C, n (%)	62 (29.0)[a]	97 (36.5)[a]	120 (33.8)[a]	72 (36.7)[a]	89 (48.4)[b]	0.0015**

Values are mean ± SEM or n (%).

Initiation of compaction (tSC), completion of compaction process (tM), initiation of blastulation (tSB) and formation of full (tB) and expanded (tEB) blastocyst; FCM: fully compacted morula; Exc-PCM: partially compacted morula with excluded cells; Ext-PCM: partially compacted morula with extruded cells; Exc/Ext-PCM: partially compacted morula with both excluded and extruded cells.

[a–c]Different superscript letters indicate a significant difference at $P < 0.05$.

*Mann–Whitney *U* test.

**Chi-squared test.

Furthermore, detailed annotation data on morphokinetics and morphological alterations revealed that AMA significantly affected the developmental events of human embryos during fertilization, compaction, and blastulation, but not blastomere cleavage. We also determined the presence and localization of cell polarization regulators, YAP and PKCζ (Coticchio et al., 2019; Gerri et al., 2020), whose patterns during compaction were significantly altered by maternal ageing.

First, we analysed the correlation between AMA and morphokinetics before the first cytokinesis, i.e. during fertilization, which has not been reported previously. PN morphology is associated with developmental competence of human embryos (Gianaroli et al., 2003). In particular, the sizes of two PNs and their relative difference are reportedly predictive of developmental competence, pregnancy outcomes, and embryo ploidy (Munne and Cohen, 1998; Zollner et al., 2002; Gamiz et al., 2003; Nagy et al., 2003; Scott, 2003). In this study, we found that the female PN size significantly decreased with maternal ageing, but the male PN size did not. This difference may be relevant to the decreased outcomes in women of AMA, although the underpinning mechanisms are not clear. However, a previous study suggested that nuclear size may reflect the chromosome content; the size of nuclei with missing chromosomes was smaller than that of the nuclei with extra chromosomes (Agerholm et al., 2008). In addition, PN size might depend on the ratio between the amount of chromatin organized in the PN and cytoplasm volume (Okajima et al., 2022). Furthermore, PN size is regulated by the amount of zygotic nuclear filamentous actin (Okuno et al., 2020). This finding supports the realization of future studies investigating the influence of maternal ageing on the status of chromatin or nuclear actin in human zygotes.

The clustering and alignment of NPBs in the area of PN juxtaposition reflect accurately the distribution of PN chromatin; therefore, the observation of non-invasive NPB provides reliable information on chromatin distribution (Cavazza et al., 2021). Once PN envelopes dissolve in preparation for the first mitosis, a correct chromatin arrangement is crucial to assist the capture of chromosomes by the kinetochore fibres of the mitotic spindle and their correct recruitment on the metaphase plate (Cavazza et al., 2021; Ezoe et al., 2022d). In the present study, decreased NPB alignment in female PN and its increased asynchronous breakdown were observed in women of AMA. This result suggests that maternal ageing adversely impacts chromatin clustering at the interface between PNs, especially in the female PN, which might lead to the failure of chromosome recruitment by kinetochore fibres. Furthermore, prolonged mitosis and asynchronous PN breakdown are typically linked to an abnormal state of nucleolus clustering—i.e. asynchronous NPB alignment and errors in chromosome capture—resulting in chromosome segregation errors and micronuclei formation (Cavazza et al., 2021). Therefore, incomplete chromatin migration and clustering before PN breakdown, especially in the female PN, could be another significant cause of AMA-derived embryo aneuploidy. Further studies evaluating the association between AMA-related abnormal PN behaviour and embryo ploidy are needed.

Blastomere compaction, which initiates at the 12- to 13-cell stage (Coticchio et al., 2021b), is the first morphogenetic event occurring in preparation for blastocyst formation and coincides with the first decision of lineage specification. Maternal ageing was also correlated with the prolongated time required for embryo compaction (TI from t8 to tSC), in which the embryo undergoes profound changes in metabolism owing to energy-demanding processes, and cellular/intercellular organization (Coticchio et al., 2021a). This process is crucial for subsequent development. In fact, our data demonstrated that both shortening (early compaction) and prolongation (delayed compaction) of this duration resulted in the impairment of blastocyst formation and embryo quality. During compaction, outer cells acquire an apical-basal cell polarity and the expression of PKCζ at the contact-free domain that inhibits the Hippo signalling pathway and its nuclear expression effectors, YAP (Ota and Sasaki, 2008; Zhao et al., 2008; Hirate et al., 2013; Gerri et al., 2020). Our results further demonstrated that embryos from women of AMA exhibited decreased PKCζ protein and a lower YAP positivity rate in the outer cells of morula, as compared to embryos from young women. It is plausible that insufficient regulation of cell polarity leads to an extension of the time required for embryo compaction. Some blastomeres, also in the fully compacted morula, did not exhibit YAP protein in either the young women or women of AMA. Interestingly, the incidence of this phenomenon was significantly higher in women of AMA than in young women. The aberrant expression of cell polarity markers might be one of the reasons for blastomere extrusion after the establishment of embryonic compaction, especially in women with AMA. Previous studies hypothesized that blastomere exclusion before compaction may be a self-correction mechanism to eliminate or reduce the proportion of the chromosomally abnormal cells, while blastomere extrusion post compaction does not exhibit the obvious correlation with embryo aneuploidy (Lagalla et al., 2017, 2020). In the present study, we confirmed the increased incidence of blastomere extrusion in women of AMA, in addition to suggesting that abnormal cells were potentially excluded/extruded by the embryos during compaction owing to either an active mechanism of self-correction or some inherent issue hampering their inclusion in the body of the embryo proper. More basic research is certainly needed to shed light on this fascinating area of investigation.

We confirmed an increased rate of embryo arrest at the morula stage in women of AMA, which is consistent with previous studies (Janny and Menezo, 1996; Pantos et al., 1999). Furthermore, the time required for blastocyst expansion (TI from tB to tEB) was also prolonged with maternal ageing; this also validates previous study findings (Kirkegaard et al., 2016; Barrie et al., 2021; Lebovitz et al., 2021). In addition, the morphological grades of ICM and TE were impaired in embryos from women of AMA. As the expansion of the blastocoel cavity requires cellular Na/K-ATPase activity and high levels of ATP (Watson, 1992), prolonged blastulation and poor morphology might be associated with AMA-related mitochondrial dysfunction. Mitochondrial activation is required for Ca^{2+} signalling and the regulation of intracellular redox potential during fertilization and embryonic development (Dumollard et al., 2007a,b); this activity progressively declines with maternal ageing, leading to reduced ATP and metabolic activity in aged oocytes (Wilding et al., 2001; Van Blerkom, 2011; Eichenlaub-Ritter, 2012).

As described above, AMA affects fertilization, compaction and blastocyst formation, but not cleavage. It remains unclear as to why errors at fertilization remain cryptic during cleavage, but 're-emerge' during morula formation. To validate our findings and speculations, molecular studies are needed, especially to reveal the association between AMA and size and asynchronous breakdown of PN, NPB alignment and subsequent development. A possible explanation to this phenomenology is that AMA-associated mitotic errors occurring at the fertilization-first cleavage transition do not disrupt cell division, but cause perturbations

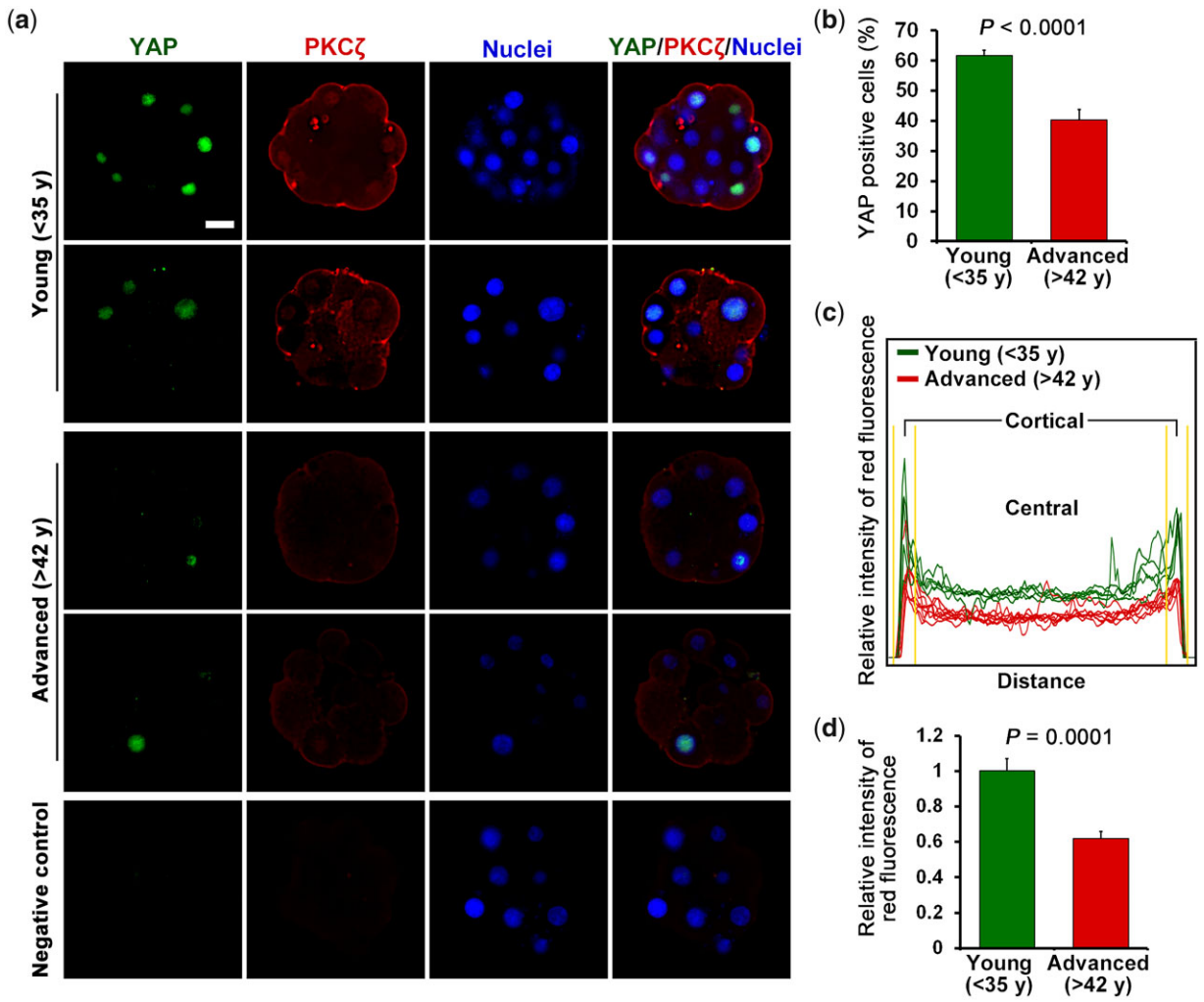

Figure 1. Immunofluorescent detection of Yes-associated protein (YAP) and protein kinase C-ζ (PKCζ) in human embryos at the morula stage. (**a**) Distribution of YAP and PKCζ in the morulae from young (<35 years, n = 10) and advanced age (>42 years, n = 10) patients. Green and red fluorescence indicate YAP and PKCζ, respectively. Scale bars represent 20 µm. (**b**) The rate of YAP-positive cells in the outer cells of the morula. The statistical analysis was performed using Student's *t*-test. (**c**) The line-scan profile of red fluorescence (PKCζ,) in the morula. The left and right ends of the profile indicate the cortical region of the outer cells in the morula. (**d**) Relative intensity of red fluorescence (PKCζ) in the cortical region in the morula (reference, young group). The statistical analysis was performed using Student's *t*-test. Error bars represent the SEM.

of the compaction process consistent with the elimination of abnormal cells.

Our study assessed the association between AMA and detailed data obtained through manual annotation of embryo morphokinetic parameters. These data strongly indicate that AMA significantly affects embryo development during fertilization, compaction, and blastulation, and highlight the need for further studies. Furthermore, in the present study, all embryos were derived from oocytes retrieved in a CC-based minimal stimulation cycle, that is, all embryos were exposed to a single treatment. This consistency allows for the exclusion of the effects of ovarian stimulation that can affect embryonic morphokinetics (Munoz *et al.*, 2012). However, our study has limitations, such as its retrospective design. In addition, paternal factors were not specifically investigated in this study. Maternal age significantly impacts PN behaviour, which, however, is also affected by the sperm aster (Reinsch and Gonczy, 1998; Roegiers *et al.*, 1999; Paix *et al.*, 2011); therefore, considering paternal age and semen quality would be valuable in further studies. In the present study, the embryonic gender was not considered. A recent study reported that embryos of different sexes display differences in timing of the appearance of male PN and the position of PN juxtaposition (Orevich *et al.*, 2022). However, they also reported that embryonic gender was not associated with the PN area and NPB alignment that were found to be associated with maternal ageing in the present study. Furthermore, we only studied ICSI-derived embryos; analysing conventional IVF-derived embryos would contribute to the accumulation of knowledge on the developmental differences

between embryos from young women and those of AMA. Moreover, the number of embryos used for the immunofluorescence analysis might be too small to firmly conclude the association between maternal ageing and decreased cell polarity during compaction; therefore, further studies are required to confirm our findings. However, we trust that our preliminary observations are significant because they suggest a novel hypothesis on the effects of maternal ageing on embryo development.

Conclusion

This study revealed that maternal ageing significantly affects PN size and intra- and extra-nuclear dynamics during fertilization. It also has an impact on the regulation of cell polarity during compaction and expansion of the blastocoel cavity during the blastocyst stage. Collectively, this evidence suggests that AMA may affect embryo competence irrespective of the well-established consequences of female meiotic errors. This indicates new avenues of research to shed new light on the mechanisms causing the AMA-related developmental decline of human embryos.

Supplementary data

Supplementary data are available at *Human Reproduction* online.

Data availability

The data underlying this study will be shared upon reasonable request to the corresponding author.

Authors' roles

K.E.: study design, experiments, data production; data interpretation; manuscript writing and revision; T.M.: data collection and experiments; H.A.: data collection; K.S.: data collection; T.T.: data collection; Y.T.: data collection; A.A.: data collection; A.S.: data collection; M.M.: data collection; S.K.: data collection; S.U.: manuscript revision; G.C.: data interpretation and manuscript writing and revision; D.C.: data interpretation and manuscript writing and revision; A.B.: manuscript revision; L.R.: manuscript revision; and K.K.: manuscript revision.

Funding

This study was supported by the participating institutions.

Conflict of interest

The authors have no conflicts of interest to declare.

References

Abe T, Yabuuchi A, Ezoe K, Skaletsky H, Fukuda J, Ueno S, Fan Y, Goldsmith S, Kobayashi T, Silber S *et al.* Success rates in minimal stimulation cycle IVF with clomiphene citrate only. *J Assist Reprod Genet* 2020;**37**:297–304.

Agerholm IE, Hnida C, Cruger DG, Berg C, Bruun-Petersen G, Kolvraa S, Ziebe S. Nuclei size in relation to nuclear status and aneuploidy rate for 13 chromosomes in donated four cells embryos. *J Assist Reprod Genet* 2008;**25**:95–102.

Barrie A, McDowell G, Troup S. An investigation into the effect of potential confounding patient and treatment parameters on human embryo morphokinetics. *Fertil Steril* 2021;**115**:1014–1022.

Bebbere D, Coticchio G, Borini A, Ledda S. Oocyte aging: looking beyond chromosome segregation errors. *J Assist Reprod Genet* 2022;**39**:793–800.

Capalbo A, Hoffmann ER, Cimadomo D, Ubaldi FM, Rienzi L. Human female meiosis revised: new insights into the mechanisms of chromosome segregation and aneuploidies from advanced genomics and time-lapse imaging. *Hum Reprod Update* 2017;**23**:706–722.

Cavazza T, Takeda Y, Politi AZ, Aushev M, Aldag P, Baker C, Choudhary M, Bucevicius J, Lukinavicius G, Elder K *et al.* Parental genome unification is highly error-prone in mammalian embryos. *Cell* 2021;**184**:2860–2877.e22.

Cimadomo D, Fabozzi G, Vaiarelli A, Ubaldi N, Ubaldi FM, Rienzi L. Impact of maternal age on oocyte and embryo competence. *Front Endocrinol (Lausanne)* 2018;**9**:327.

Ciray HN, Campbell A, Agerholm IE, Aguilar J, Chamayou S, Esbert M, Sayed S; Time-Lapse User Group. Proposed guidelines on the nomenclature and annotation of dynamic human embryo monitoring by a time-lapse user group. *Hum Reprod* 2014;**29**:2650–2660.

Coticchio G, Barrie A, Lagalla C, Borini A, Fishel S, Griffin D, Campbell A. Plasticity of the human preimplantation embryo: developmental dogmas, variations on themes and self-correction. *Hum Reprod Update* 2021a;**27**:848–865.

Coticchio G, Ezoe K, Lagalla C, Shimazaki K, Ohata K, Ninomiya M, Wakabayashi N, Okimura T, Uchiyama K, Kato K *et al.* Perturbations of morphogenesis at the compaction stage affect blastocyst implantation and live birth rates. *Hum Reprod* 2021b;**36**:918–928.

Coticchio G, Lagalla C, Sturmey R, Pennetta F, Borini A. The enigmatic morula: mechanisms of development, cell fate determination, self-correction and implications for ART. *Hum Reprod Update* 2019;**25**:422–438.

Coticchio G, Mignini Renzini M, Novara PV, Lain M, De Ponti E, Turchi D, Fadini R, Dal Canto M. Focused time-lapse analysis reveals novel aspects of human fertilization and suggests new parameters of embryo viability. *Hum Reprod* 2018;**33**:23–31.

Coughlan C, Ledger W, Wang Q, Liu F, Demirol A, Gurgan T, Cutting R, Ong K, Sallam H, Li TC. Recurrent implantation failure: definition and management. *Reprod Biomed Online* 2014;**28**:14–38.

Diez-Juan A, Rubio C, Marin C, Martinez S, Al-Asmar N, Riboldi M, Diaz-Gimeno P, Valbuena D, Simon C. Mitochondrial DNA content as a viability score in human euploid embryos: less is better. *Fertil Steril* 2015;**104**:534–541.e1.

Dumollard R, Duchen M, Carroll J. The role of mitochondrial function in the oocyte and embryo. *Curr Top Dev Biol* 2007a;**77**:21–49.

Dumollard R, Ward Z, Carroll J, Duchen MR. Regulation of redox metabolism in the mouse oocyte and embryo. *Development* 2007b;**134**:455–465.

Duncan FE, Jasti S, Paulson A, Kelsh JM, Fegley B, Gerton JL. Age-associated dysregulation of protein metabolism in the mammalian oocyte. *Aging Cell* 2017;**16**:1381–1393.

Ebner T, Moser M, Shebl O, Sommergruber M, Gaiswinkler U, Tews G. Morphological analysis at compacting stage is a valuable prognostic tool for ICSI patients. *Reprod Biomed Online* 2009;**18**:61–66.

Eichenlaub-Ritter U. Oocyte ageing and its cellular basis. *Int J Dev Biol* 2012;**56**:841–852.

ESHRE Capri Workshop Group. Genetic aspects of female reproduction. *Hum Reprod Update* 2008;**14**:293–307.

ESHRE Working group on Time-lapse technology. Good practice recommendations for the use of time-lapse technology. *Hum Reprod Open* 2020;**2020**:hoaa008.

Ezoe K, Coticchio G, Takenouchi H, Taoda S, Namerikawa S, Honda K, Miki T, Okimura T, Kobayashi T, Borini A *et al.* Spatiotemporal perturbations of pronuclear breakdown preceding syngamy affect early human embryo development: a retrospective observational study. *J Assist Reprod Genet* 2022a;**39**:75–84.

Ezoe K, Fukuda J, Takeshima K, Shinohara K, Kato K. Letrozole-induced endometrial preparation improved the pregnancy outcomes after frozen blastocyst transfer compared to the natural cycle: a retrospective cohort study. *BMC Pregnancy Childbirth* 2022b;**22**:824.

Ezoe K, Hickman C, Miki T, Okimura T, Uchiyama K, Yabuuchi A, Kobayashi T, Coticchio G, Kato K. Cytoplasmic halo characteristics during fertilization and their implications for human preimplantation embryo development and pregnancy outcome. *Reprod Biomed Online* 2020;**41**:191–202.

Ezoe K, Miki T, Ohata K, Fujiwara N, Yabuuchi A, Kobayashi T, Kato K. Prolactin receptor expression and its role in trophoblast outgrowth in human embryos. *Reprod Biomed Online* 2021a;**42**:699–707.

Ezoe K, Miki T, Okimura T, Uchiyama K, Yabuuchi A, Kobayashi T, Kato K. Characteristics of the cytoplasmic halo during fertilisation correlate with the live birth rate after fresh cleaved embryo transfer on day 2 in minimal ovarian stimulation cycles: a retrospective observational study. *Reprod Biol Endocrinol* 2021b;**19**:172.

Ezoe K, Ohata K, Morita H, Ueno S, Miki T, Okimura T, Uchiyama K, Yabuuchi A, Kobayashi T, Montag M *et al.* Prolonged blastomere movement induced by the delay of pronuclear fading and first cell division adversely affects pregnancy outcomes after fresh embryo transfer on Day 2: a time-lapse study. *Reprod Biomed Online* 2019;**38**:659–668.

Ezoe K, Shimazaki K, Miki T, Takahashi T, Tanimura Y, Amagai A, Sawado A, Akaike H, Mogi M, Kaneko S *et al.* Association between a deep learning-based scoring system with morphokinetics and morphological alterations in human embryos. *Reprod Biomed Online* 2022c;**45**:1124–1132.

Ezoe K, Takahashi T, Shimazaki K, Miki T, Tanimura Y, Amagai A, Sawado A, Akaike H, Mogi M, Kaneko S *et al.* Human 1PN and 3PN zygotes recapitulate all morphokinetic events of normal fertilization but reveal novel developmental errors. *Hum Reprod* 2022d;**37**:2307–2319.

Faramarzi A, Khalili MA, Mangoli E. Correlations between embryo morphokinetic development and maternal age: results from an intracytoplasmic sperm injection program. *Clin Exp Reprod Med* 2019;**46**:119–124.

Franasiak JM, Forman EJ, Hong KH, Werner MD, Upham KM, Treff NR, Scott RT Jr. The nature of aneuploidy with increasing age of the female partner: a review of 15,169 consecutive trophectoderm biopsies evaluated with comprehensive chromosomal screening. *Fertil Steril* 2014;**101**:656–663.e1.

Gamiz P, Rubio C, de los Santos MJ, Mercader A, Simon C, Remohi J, Pellicer A. The effect of pronuclear morphology on early development and chromosomal abnormalities in cleavage-stage embryos. *Hum Reprod* 2003;**18**:2413–2419.

Gardner D, Schoolcraft W. *In Vitro Culture of Human Blastocyst. Towards Reproductive Certainty: Infertility and Genetics Beyond*. Carnforth: Parthenon Press, 1999.

Gerri C, McCarthy A, Alanis-Lobato G, Demtschenko A, Bruneau A, Loubersac S, Fogarty NME, Hampshire D, Elder K, Snell P *et al.* Initiation of a conserved trophectoderm program in human, cow and mouse embryos. *Nature* 2020;**587**:443–447.

Gianaroli L, Magli MC, Ferraretti AP, Fortini D, Grieco N. Pronuclear morphology and chromosomal abnormalities as scoring criteria for embryo selection. *Fertil Steril* 2003;**80**:341–349.

Gruhn JR, Zielinska AP, Shukla V, Blanshard R, Capalbo A, Cimadomo D, Nikiforov D, Chan AC, Newnham LJ, Vogel I *et al.* Chromosome errors in human eggs shape natural fertility over reproductive life span. *Science* 2019;**365**:1466–1469.

Heffner LJ. Advanced maternal age—how old is too old? *N Engl J Med* 2004;**351**:1927–1929.

Hirate Y, Hirahara S, Inoue K, Suzuki A, Alarcon VB, Akimoto K, Hirai T, Hara T, Adachi M, Chida K *et al.* Polarity-dependent distribution of angiomotin localizes Hippo signaling in preimplantation embryos. *Curr Biol* 2013;**23**:1181–1194.

Janny L, Menezo YJ. Maternal age effect on early human embryonic development and blastocyst formation. *Mol Reprod Dev* 1996;**45**:31–37.

Karakida S, Ezoe K, Fukuda J, Yabuuchi A, Kobayashi T, Kato K. Effects of gonadotropin administration on clinical outcomes in clomiphene citrate-based minimal stimulation cycle IVF. *Reprod Med Biol* 2020;**19**:128–134.

Kato K, Ezoe K, Yabuuchi A, Fukuda J, Kuroda T, Ueno S, Fujita H, Kobayashi T. Comparison of pregnancy outcomes following fresh and electively frozen single blastocyst transfer in natural cycle and clomiphene-stimulated IVF cycles. *Hum Reprod Open* 2018;**2018**:hoy006.

Kato K, Ueno S, Yabuuchi A, Uchiyama K, Okuno T, Kobayashi T, Segawa T, Teramoto S. Women's age and embryo developmental speed accurately predict clinical pregnancy after single vitrified-warmed blastocyst transfer. *Reprod Biomed Online* 2014;**29**:411–416.

Keefe DL, Niven-Fairchild T, Powell S, Buradagunta S. Mitochondrial deoxyribonucleic acid deletions in oocytes and reproductive aging in women. *Fertil Steril* 1995;**64**:577–583.

Kirkegaard K, Sundvall L, Erlandsen M, Hindkjær JJ, Knudsen UB, Ingerslev HJ. Timing of human preimplantation embryonic development is confounded by embryo origin. *Hum Reprod* 2016;**31**:324–331.

Kola I, Trounson A, Dawson G, Rogers P. Tripronuclear human oocytes: altered cleavage patterns and subsequent karyotypic analysis of embryos. *Biol Reprod* 1987;**37**:395–401.

Lagalla C, Coticchio G, Sciajno R, Tarozzi N, Zaca C, Borini A. Alternative patterns of partial embryo compaction: prevalence, morphokinetic history and possible implications. *Reprod Biomed Online* 2020;**40**:347–354.

Lagalla C, Tarozzi N, Sciajno R, Wells D, Di Santo M, Nadalini M, Distratis V, Borini A. Embryos with morphokinetic abnormalities may develop into euploid blastocysts. *Reprod Biomed Online* 2017; **34**:137–146.

Lebovitz O, Michaeli M, Aslih N, Poltov D, Estrada D, Atzmon Y, Shalom-Paz E. Embryonic development in relation to maternal age and conception probability. *Reprod Sci* 2021;**28**:2292–2300.

Martinez M, Santalo J, Rodriguez A, Vassena R. High reliability of morphokinetic annotations among embryologists. *Hum Reprod Open* 2018;**2018**:hoy009.

Mazzilli R, Cimadomo D, Vaiarelli A, Capalbo A, Dovere L, Alviggi E, Dusi L, Foresta C, Lombardo F, Lenzi A *et al*. Effect of the male factor on the clinical outcome of intracytoplasmic sperm injection combined with preimplantation aneuploidy testing: observational longitudinal cohort study of 1,219 consecutive cycles. *Fertil Steril* 2017;**108**:961–972.e3.

Mills M, Rindfuss RR, McDonald P, Te Velde E; ESHRE Reproduction and Society Task Force. Why do people postpone parenthood? Reasons and social policy incentives. *Hum Reprod Update* 2011;**17**: 848–860.

Mori C, Yabuuchi A, Ezoe K, Murata N, Takayama Y, Okimura T, Uchiyama K, Takakura K, Abe H, Wada K *et al*. Hydroxypropyl cellulose as an option for supplementation of cryoprotectant solutions for embryo vitrification in human assisted reproductive technologies. *Reprod Biomed Online* 2015;**30**:613–621.

Morimoto N, Hashimoto S, Yamanaka M, Nakano T, Satoh M, Nakaoka Y, Iwata H, Fukui A, Morimoto Y, Shibahara H. Mitochondrial oxygen consumption rate of human embryos declines with maternal age. *J Assist Reprod Genet* 2020;**37**: 1815–1821.

Mosher WD, Pratt WF. Fecundity and infertility in the United States: incidence and trends. *Fertil Steril* 1991;**56**:192–193.

Munne S, Cohen J. Chromosome abnormalities in human embryos. *Hum Reprod Update* 1998;**4**:842–855.

Munoz M, Cruz M, Humaidan P, Garrido N, Perez-Cano I, Meseguer M. Dose of recombinant FSH and oestradiol concentration on day of HCG affect embryo development kinetics. *Reprod Biomed Online* 2012;**25**:382–389.

Nagy ZP, Dozortsev D, Diamond M, Rienzi L, Ubaldi F, Abdelmassih R, Greco E. Pronuclear morphology evaluation with subsequent evaluation of embryo morphology significantly increases implantation rates. *Fertil Steril* 2003;**80**:67–74.

Nelson SM, Lawlor DA. Predicting live birth, preterm delivery, and low birth weight in infants born from in vitro fertilisation: a prospective study of 144,018 treatment cycles. *PLoS Med* 2011;**8**: e1000386.

Ohata K, Ezoe K, Miki T, Kouraba S, Fujiwara N, Yabuuchi A, Kobayashi T, Kato K. Effects of fatty acid supplementation during vitrification and warming on the developmental competence of mouse, bovine and human oocytes and embryos. *Reprod Biomed Online* 2021;**43**:14–25.

Ohata K, Ezoe K, Miki T, Morita H, Tsuchiya R, Kaneko S, Okimura T, Uchiyama K, Yabuuchi A, Kobayashi T *et al*. Blastomere movement post first cell division correlates with embryonic compaction and subsequent blastocyst formation. *Reprod Biol Endocrinol* 2019; **17**:44.

Okajima N, Xiao W, Lopata A, Sankai T, Yasmin L, Nagai Y, Okamoto R, Tasaki H, Otsuki J. Nuclear-to-cytoplasmic ratios of 1PN and 2PN zygotes after in vitro fertilization of mouse oocytes. *Zygote* 2022;**30**:120–124.

Okuno T, Li WY, Hatano Y, Takasu A, Sakamoto Y, Yamamoto M, Ikeda Z, Shindo T, Plessner M, Morita K *et al*. Zygotic nuclear F-actin safeguards embryonic development. *Cell Rep* 2020;**31**: 107824.

Orevich LS, Watson K, Ong K, Korman I, Turner R, Shaker D, Liu Y. Morphometric and morphokinetic differences in the sperm- and oocyte-originated pronuclei of male and female human zygotes: a time-lapse study. *J Assist Reprod Genet* 2022;**39**:97–106.

Ota M, Sasaki H. Mammalian Tead proteins regulate cell proliferation and contact inhibition as transcriptional mediators of Hippo signaling. *Development* 2008;**135**:4059–4069.

Paix A, Le Nguyen PN, Sardet C. Bi-polarized translation of ascidian maternal mRNA determinant pem-1 associated with regulators of the translation machinery on cortical Endoplasmic Reticulum (cER). *Dev Biol* 2011;**357**:211–226.

Pantos K, Athanasiou V, Stefanidis K, Stavrou D, Vaxevanoglou T, Chronopoulou M. Influence of advanced age on the blastocyst development rate and pregnancy rate in assisted reproductive technology. *Fertil Steril* 1999;**71**:1144–1146.

Ramalho-Santos J, Varum S, Amaral S, Mota PC, Sousa AP, Amaral A. Mitochondrial functionality in reproduction: from gonads and gametes to embryos and embryonic stem cells. *Hum Reprod Update* 2009;**15**:553–572.

Reinsch S, Gonczy P. Mechanisms of nuclear positioning. *J Cell Sci* 1998;**111**:2283–2295.

Roegiers F, Djediat C, Dumollard R, Rouviere C, Sardet C. Phases of cytoplasmic and cortical reorganizations of the ascidian zygote between fertilization and first division. *Development* 1999;**126**: 3101–3117.

Rubio I, Kuhlmann R, Agerholm I, Kirk J, Herrero J, Escriba MJ, Bellver J, Meseguer M. Limited implantation success of direct-cleaved human zygotes: a time-lapse study. *Fertil Steril* 2012;**98**: 1458–1463.

Schmidt L, Sobotka T, Bentzen JG, Nyboe Andersen A; ESHRE Reproduction and Society Task Force. Demographic and medical consequences of the postponement of parenthood. *Hum Reprod Update* 2012;**18**:29–43.

Scott L. Pronuclear scoring as a predictor of embryo development. *Reprod Biomed Online* 2003;**6**:201–214.

Sundvall L, Ingerslev HJ, Breth Knudsen U, Kirkegaard K. Inter- and intra-observer variability of time-lapse annotations. *Hum Reprod* 2013;**28**:3215–3221.

Toner JP, Coddington CC, Doody K, Van Voorhis B, Seifer DB, Ball GD, Luke B, Wantman E. Society for Assisted Reproductive Technology and assisted reproductive technology in the United States: a 2016 update. *Fertil Steril* 2016;**106**:541–546.

Ubaldi FM, Cimadomo D, Capalbo A, Vaiarelli A, Buffo L, Trabucco E, Ferrero S, Albani E, Rienzi L, Levi Setti PE. Preimplantation genetic diagnosis for aneuploidy testing in women older than 44 years: a multicenter experience. *Fertil Steril* 2017;**107**:1173–1180.

Ueno S, Ezoe K, Abe T, Yabuuchi A, Uchiyama K, Okuno T, Kobayashi T, Kato K. Maternal age and initial beta-hCG levels

predict pregnancy outcome after single vitrified-warmed blastocyst transfer. *J Assist Reprod Genet* 2014;**31**:1175–1181.

Van Blerkom J. Mitochondrial function in the human oocyte and embryo and their role in developmental competence. *Mitochondrion* 2011;**11**:797–813.

Warshaviak M, Kalma Y, Carmon A, Samara N, Dviri M, Azem F, Ben-Yosef D. The effect of advanced maternal age on embryo morphokinetics. *Front Endocrinol (Lausanne)* 2019;**10**:686.

Watson AJ. The cell biology of blastocyst development. *Mol Reprod Dev* 1992;**33**:492–504.

Wilding M, Dale B, Marino M, di Matteo L, Alviggi C, Pisaturo ML, Lombardi L, De Placido G. Mitochondrial aggregation patterns and activity in human oocytes and preimplantation embryos. *Hum Reprod* 2001;**16**:909–917.

Zhao B, Ye X, Yu J, Li L, Li W, Li S, Yu J, Lin JD, Wang CY, Chinnaiyan AM *et al*. TEAD mediates YAP-dependent gene induction and growth control. *Genes Dev* 2008;**22**:1962–1971.

Zollner U, Zollner KP, Hartl G, Dietl J, Steck T. The use of a detailed zygote score after IVF/ICSI to obtain good quality blastocysts: the German experience. *Hum Reprod* 2002;**17**:1327–1333.